Proceedings of ASME Turbo Expo 2011
GT2011
June 6-10, 2011, Vancouver, British Columbia, Canada

GT2011-46204

NUMERICAL ANALYSIS OF THREE-DIMENSIONAL TURBINE AIRFOIL DESIGNS

Thorsten Poehler*

Peter Jeschke

Institute of Jet Propulsion and Turbomachinery
RWTH Aachen University
Templergraben 55, 52062 Aachen, Germany
poehler@ist.rwth-aachen.de

Yavuz Guendogdu

Jochen Gier

MTU Aero Engines GmbH
Dachauer Strasse 665
80955 Munich, Germany

ABSTRACT

In this paper the analysis of CFD results of three-dimensional turbine stator vane designs combined with non-axisymmetric endwalls is presented. A Design of Experiments (DoE) method has been used to generate 120 different combinations of the geometrical parameters. By means of a statistical approach the generic correlations and sensitivities of geometrical parameters on the aerodynamic behavior of three-dimensional turbine airfoils are demonstrated. The interpretation of the correlations leads to the finding, that different parameters of the three-dimensional shape fulfill different tasks. The reduction of turbulent kinetic energy and secondary kinetic energy are particularly sensitive to different geometrical parameters.

By means of the same statistical approach it is also shown that for three-dimensional designs a distinction should be made between losses that occur within the vane passage and losses expected to arise downstream of the evaluation plane. By consideration of this distinction four modified designs have been chosen for a more detailed analysis. The results indicate that the losses produced by the secondary flow can be diminished by means of a three-dimensional shape of the turbine vane. However, this leads to increasing losses occurring at the laminar-turbulent separation bubble on the suction side of the vane. Therefore, non-axisymmetric endwall contouring should be implemented early in the design process to compensate this behavior by adapting the profile pressure distribution.

* Address all correspondence to this author.

NOMENCLATURE

c	velocity vector
DoE	Design of Experiments
h	passage height
k	turbulent kinetic energy
l	chord length
KE	kinetic energy
PKE	primary kinetic energy
p	pitch length
r	correlation parameter
R	geometrical contour parameter
Re	Reynolds number
SKE	secondary kinetic energy
span	passage height
T	static temperature
TKE	turbulent kinetic energy
WA	wedge angle at leading edge
X	axial coordinate
y^+	dimensionless wall scale

Subscripts

hub	hub
io	difference between outlet and inlet
is	isentropic
loss	difference to isentropic process
norm	normalized (concerning passage height and axial vane chord respectively)
prim	primary flow
shr	shroud

Greek symbols

γ	turbulence intermittency
θ	boundary layer momentum thickness
ω	characteristic turbulent frequency, total pressure loss coefficient

INTRODUCTION

In the recent years three-dimensional vane designs have been intensively investigated. Non-axisymmetric endwall contours have in particular gained the center stage of researchers focus. The basic idea of non-axisymmetric endwall contouring is an acceleration of the endwall flow by a concave endwall curvature near the pressure side and a deceleration by a convex endwall curvature at the suction side of the vane. Due to this design modification the cross-passage pressure gradient can be reduced. Since the cross passage pressure gradient is causative for the passage vortex, secondary flow can be effectively reduced by means of non-axisymmetric endwall contours. The concept was shown by Rose [1], who demonstrated the capability of non-axisymmetric endwall contouring.

The research on the design concept of non-axisymmetric endwalls has been intensely pursued. Harvey et al. [2] developed two designs and showed that the distribution of static pressure as well as the exit angle deviations can be positively affected. In this manner the secondary kinetic energy has been reduced by 40% at constant total pressure loss. Hartland and Gregory-Smith [3] used a design system for non-axisymmetric endwall contours based on the camber line of the vane resulting in a reduction of the secondary flow coefficient of about 61%. Additional results have been demonstrated by Ingram et al. [4]. Although a separation bubble occurred at the endwall, it has been detected that the secondary kinetic energy has been reduced.

The results investigated with the Durham Cascade have been applied to the design of the turbine vanes of the Rolls Royce Trent 500 resulting in a numerical efficiency improvement of 0.4%. The experiments showed an increase in efficiency by 0.59% [5, 6] for the high pressure turbine and 0.9% for the intermediate pressure turbine [7].

The combination of non-axisymmetric endwall contours with a three-dimensional turbine vane design has been shown by Pioske [8], Nagel et al. [9], and Nagel and Baier [10]. The results of Pioske [8] led to the conclusion, that a homogenization of the exit flow angle does not consequently results in an improvement of the stage efficiency. By utilizing a optimization process based on a sequential quadratic programming method, Nagel and Baier [10] designed a shape featuring a reduction of the secondary kinetic energy by 60% and a decreased total pressure loss of 22%.

At the 1.5 stage turbine LISA of the ETH Zurich two non-axisymmetric endwall profiles have been analyzed in detail by Schuepbach et al. [11]. The results have shown, that a reduction of secondary kinetic energy does not necessarily leads to a loss improvement.

The three-dimensional vane designs presented in this paper are based on the geometry of the Aachen cold air turbine. In a former paper it has been shown by a detailed numerical analysis, that the secondary flow of the first vane can effectively be reduced by means of a non-axisymmetric endwall shape [12]. For the combination of non-axisymmetric endwalls and vane profile modifications the more generic approach of statistical analysis has been chosen to identify the important geometrical parameters. The effect of three-dimensional vane designs on the loss production is demonstrated by an analysis of four representative designs.

DESIGN SUBJECT

The three-dimensional vane designs presented in this paper have been designed for the first stator of a 1.5-stage axial flow turbine (represented in fig. 1). The datum profiles of the turbine meets state of the art LPT designs, particularly with regard to the vane profiling and the loading. It does not feature any 3D design elements like lean, bow or sweep.

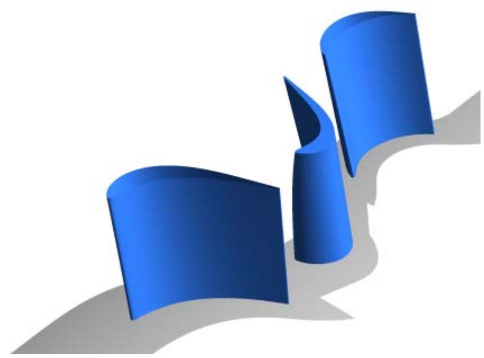

	blade #	p/l	h/l	Zweifel Number
stator 1	33	0,9	0,95	0,79
rotor	44	0,98	1,40	0,95
stator 2	66	0,71	1,51	0,89

Fig. 1 Blading of the 1.5-stage turbine

Operating at design conditions, the Reynolds number of the first stator, based on the exit velocity and the chord length, is 8.15×10^5, the exit Mach number is approximately 0.465.

Due to the aftloading of the profile a small separation bubble occurs on the suction side of the vane between 85% and 90% axial chord. The losses produced by the first stator in the aerodynamic design point are given in fig. 2. Depending on the definition of the SKE (see below), the losses of secondary flow downstream of the evaluation plane are only 39.0% / 23.6% / 20.6% of the mixing losses.

$T \cdot \Delta s_{io}$ [J/kg]	377.72
$T_{mix} \cdot \Delta s_{mix}$ [J/kg]	80.55
SKE [J/kg]	31.43
SKE2 [J/kg]	18.99
SKE3 [J/kg]	16.63
TKE [J/kg]	21.70

Fig. 2 Losses of the first stator

DESIGN OF EXPERIMENTS

The specification of different geometries has been conducted by utilizing a Design of Experiments method. In order to provide a sufficient database, 120 CFD calculations of the first vane with various geometries have been conducted.

The modification of the endwalls is defined by five splines orientated with the camber line (fig. 3). Each spline features four radial moveable points (green points), which are hereinafter denominated as R_A1 to R_E4. By this geometry definition very complex endwall surfaces can be designed. In order to reduce the amount of independent input parameters the hub and the shroud endwalls are modified symmetrically. In this manner combinations of beneficial and deficient contoured endwalls can also be avoided.

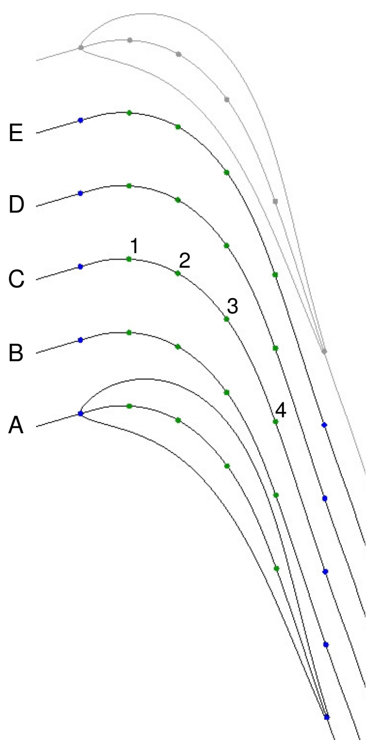

Fig. 3 Location of endwall contour parameters

Additionally, a variation of the wedge angles at the leading edge has been implemented for vane profile modifications. The wedge angles are specified at 0% and 100% of normalized span. For a smooth radial stacking a quadratic function has been used. The vane profile modifications are limited to a distance of 20% normalized span to the endwall.

The total amount of geometrical input parameters accumulates to 22. The limits have been set to ±3% span in the case of the endwall parameters and ±10% in the case of the wedge angles. A conservation of the capacity of the vane within the DoE study, e.g. by restaggering, has not been implemented. It has been experienced, that this impact is of negligible order within this study.

NUMERICAL SETUP

The numerical simulations presented in this paper have been conducted with the finite volume solver TRACE v7.1, developed by the Institute of Propulsion Technology (DLR) in cooperation with MTU Aero Engines GmbH.

The solver is based on a finite-volume approach with a cell-centered discretization. The accuracy in time and space is of second order. The closure of the RANS-equations is fulfilled by the k-ω turbulence model. Additionally, transition modeling has been applied using the γ-Re_θ differential equation model.

A detailed comparison of unsteady numerical results conducted with TRACE and experimental data for the Aachen cold air turbine is given by Restemeier et al. [13].

The flow path has been discretized using Ansys ICEM v12.1 and consists of approximately 800000 elements. Due to the requirements of the transition model the dimensionless wall scale is $y^+ \approx 1$. Therefore, a low-Reynolds approach has been used for accurate boundary layer resolution.

The aerodynamic boundary conditions are given by profiles of total pressure, total temperature, flow angle, turbulence intensity and turbulent length scale at the inlet and a radial static pressure distribution at the outlet of the computational domain.

POSTPROCESSING

In addition to common aerodynamic loss values three different definitions of the secondary kinetic energy (SKE) have been evaluated. All SKE definitions are based on a primary flow which is derived from the real flow by means of specific averaging. The axial and the radial component of the primary flow velocity are the result of a mass-weighted averaging of these variables on stripes of constant radius. For the circumferential velocity component the integral swirl is determined on stripes of constant pitchwise coordinate. Dividing the integral swirl by the radius results in a two dimensional distribution of the primary velocity component. The presented approach provides an evaluation of primary kinetic energy, which is very close to the real flow of the free vortex vane design.

Based on this definition of the primary flow, the first definition of SKE is obtained by evaluating the differences of the real flow components to the corresponding components of the averaged flow.

$$SKE = \frac{1}{2}\left[\left(c - \bar{c}\right)^2\right] \qquad \text{(eq. 1)}$$

The second and the third definition of SKE differ in the frame of reference. SKE2 is evaluated in a rotating frame of reference at aerodynamic design point, while SKE3 is formulated in the stationary frame of reference. Unlike the first SKE definition here only the direction of the primary flow is used. The specific kinetic energy of the local velocity vector component in the primary flow direction is identified as PKE2 and PKE3 respectively. The secondary kinetic energy is then derived from the difference between the kinetic energy and the primary kinetic energy.

$$SKE2 = KE_{rel} - PKE_{rel} \quad \text{(eq. 2)}$$

$$SKE3 = KE - PKE \quad \text{(eq. 3)}$$

The approach for the evaluation of the mixing losses has been described by Rose [14]. It is based on an analytical solution of the Euler equations.

The kinetic energy loss is defined as the difference between the isentropic and real enthalpy difference:

$$KE_{loss} = \Delta h_{is,io} - \Delta h_{io} \quad \text{(eq. 4)}$$

All values have been evaluated in the stator exit plane positioned 18% of axial chord downstream of the trailing edge. The difference values between inlet and outlet of the stator refer to an inlet plane positioned 200% of a axial chord upstream of the leading edge.

It is a well-known fact, that CFD is not capable to predict absolute loss values very precisely. However, CFD is also known to predict inner-numerical differences very accurately. Otherwise no gradient-based optimization would be successful. Therefore, although the differences of aerodynamic values the presented evaluations are based on are generally very small, the points made in this paper should be valid.

IMPACT OF THREEDIMENSIONAL DESIGN PARAMETERS ON THE AERODYNAMICS

The sensitivity of aerodynamic values in regard to a geometrical parameter has been evaluated by means of a Pearson correlation matrix. The correlation parameter is defined as

$$r(a,b) = \frac{\mathrm{cov}(a,b)}{\sqrt{\mathrm{var}(a) \cdot \mathrm{var}(b)}}, \quad \text{(eq. 5)}$$

where var( ) is the variance of a parameter and cov(,) is the covariance of two parameters. The correlation parameter gives values between -1 and 1, where 1 indicates a perfect positive correlation (both parameters increase or decrease symmetrically) and -1 indicates a perfect negative correlation (both parameters show a contradicting behavior). Additionally, for high values of the correlation parameter the influence of one parameter on the bandwidth of the variation of the other parameter has to be dominant. A description of the method can be found in [15].

The correlations between the geometrical and aerodynamic values associated with upstream or expectable downstream losses are shown in fig. 4. The position of the geometrical parameters has been given in fig. 3. An increase of a contour parameter corresponds to a lifting of the radial height at the hub and a lowering at the shroud and therefore is equivalent to a decreasing passage height. Values within the range of -0.15 to 0.15 are blanked due to insufficient significance.

Since the secondary flow losses are a minor part of the overall losses, the designer should start improving the design with the focus on reducing the entropy increase within the vane row. The parameters R_A2, R_B2, R_C3, R_E1 and R_E2 as well as the wedge angles are the most suitable for this task. Except for R_C3 all of these parameters are located in the first 50% of the axial chord. This is the part of the passage, where flow conditions are prearranged for the downstream part of the passage. Special attention should be paid to this region in the design process as well as in terms of manufacturing of non-axisymmetric endwalls.

Losses of secondary order are secondary kinetic energy and turbulent kinetic energy. Concerning the SKE the parameters R_A1, R_B3, R_C2, R_D2 and R_D3 can be used to effectively influence the secondary flow. These parameters are orientated with the trajectory of the pressure side leg of the horseshoe vortex. The secondary flow is also very sensitive to the parameter R_C3, but this correlation is contrary to entropy reduction. Therefore this parameter indicates a conflict between entropy loss reduction and secondary flow loss reduction.

	Δs_{io}	Δs_{mix}	m	SKE	SKE2	SKE3	TKE	ω	KE_{loss}
R_A1		-0.2		-0.3	-0.3	-0.3		-0.2	
R_A2	0.2							0.2	0.2
R_A3		-0.3		-0.2	-0.2				
R_A4									
R_B1									
R_B2	0.3		0.2			0.2		0.3	0.3
R_B3			-0.7	0.3	0.3	0.3			
R_B4						-0.2			
R_C1						0.2			
R_C2		0.3		0.2	0.3	0.3			
R_C3	-0.2	0.3	-0.2	0.4	0.4	0.3			-0.2
R_C4			-0.3						
R_D1									
R_D2		-0.2		-0.3	-0.3	-0.3	-0.3		
R_D3		-0.2	0.3	0.2	0.2	0.2			
R_D4			-0.2						
R_E1	-0.2	-0.2					-0.5	-0.2	-0.2
R_E2	-0.3	-0.4		-0.2	-0.3	-0.3	-0.4	-0.3	-0.3
R_E3									
R_E4				0.2	0.2	0.2			
WA_hub	-0.2	-0.3	-0.4	-0.2	-0.2		-0.3	-0.2	-0.2
WA_shr	-0.3	-0.2	-0.4	-0.3	-0.3	-0.3	-0.2	-0.2	-0.3

Fig. 4 Pearson correlation matrix (geometry vs. aerodynamics)

The turbulent kinetic energy is primarily influenced by the pressure side contour parameters R_E1 and R_E2. It has been found, that a shifting of the contour by these parameters initially results in an increase of the turbulence in the front part of the passage. This is due to the disturbance of the flow and the increasing cross passage flow, which is typical for non-axisymmetric endwall contours. In the middle and the rear part of the passage, the TKE is then reduced by a reduction of the skewing in the endwall boundary layers due to decreasing cross passage flow. Therefore a lifting of the endwall contour at these geometrical parameters leads to lower TKE values at the evaluation plane.

The correlations of upstream losses and the values associated with losses, which are expected to occur downstream, are given in fig. 5. In contrast to the geometric-aerodynamic correlation, where a physical distance exists between the location of the geometrical modification and the evaluation of the aerodynamic result, stronger correlations can be expected here. Additionally, there always is physical relation between the different aerodynamic values (except SKE1), which should also lead to high values of the correlation parameter. Therefore, the values given in correlation matrix have to be classified as low values.

	Δs_{mix}	SKE	SKE2	SKE3	TKE
Δs_{io}	0.5	0.5	0.5	0.5	0.7
PKE	-0.5	-0.5	-0.5	-0.6	-0.7
PKE2		-0.3	-0.3	-0.3	
PKE3	-0.4	-0.5	-0.5	-0.5	-0.7
ω	0.5	0.5	0.5	0.5	0.7
KE_{loss}	0.5	0.4	0.5	0.5	0.7

Fig. 5 Pearson correlation matrix (upstream losses vs. expectable downstream losses)

This clearly shows, that distinction should be made between upstream and expectable downstream losses.

ANALYSIS OF CHOSEN DESIGNS

From the results of the DoE study four modified designs have been chosen for a more detailed analysis. Each of the selected modified designs shows a minimum concerning different loss values. By consideration of the low correlation values shown in fig. 5, two of the selected designs feature low upstream losses (designs A and D) and the other two designs are characterized by reduced downstream losses (designs B and C). The integral results in terms of the deviation to the baseline design are given in fig. 6, the corresponding modifications of the endwall contours at the hub are depicted in fig. 7.

	Design with lowest…			
	Δs_{io}	SKE3	TKE	KE_{loss}
	Design A	Design B	Design C	Design D
Δs_{io}	-0.433%	6.456%	4.512%	0.654%
Δs_{mix}	2.736%	-2.907%	0.757%	2.441%
m	1.006%	-1.129%	0.775%	0.041%
PKE	0.035%	-0.187%	-0.167%	0.066%
PKE2	0.748%	-0.935%	0.131%	0.335%
PKE3	0.038%	-0.182%	-0.163%	0.067%
SKE	3.614%	-7.299%	1.855%	0.714%
SKE2	2.973%	-12.212%	2.481%	0.290%
SKE3	0.914%	-13.711%	2.032%	-0.834%
TKE	-1.980%	-0.794%	-3.399%	0.012%
ω	-0.142%	5.543%	3.484%	0.411%
KE_{loss}	-0.377%	7.291%	5.517%	-0.800%

Fig. 6 Integral aerodynamic values of chosen designs

The manipulation of the flow by design A showed the lowest value of the entropy difference between inlet and outlet within the DoE study, although it has been reduced only slightly. According to this the total pressure loss has also been reduced by the design. The expectable downstream losses represented by the mixing losses, turbulence values and SKE values have been increased.

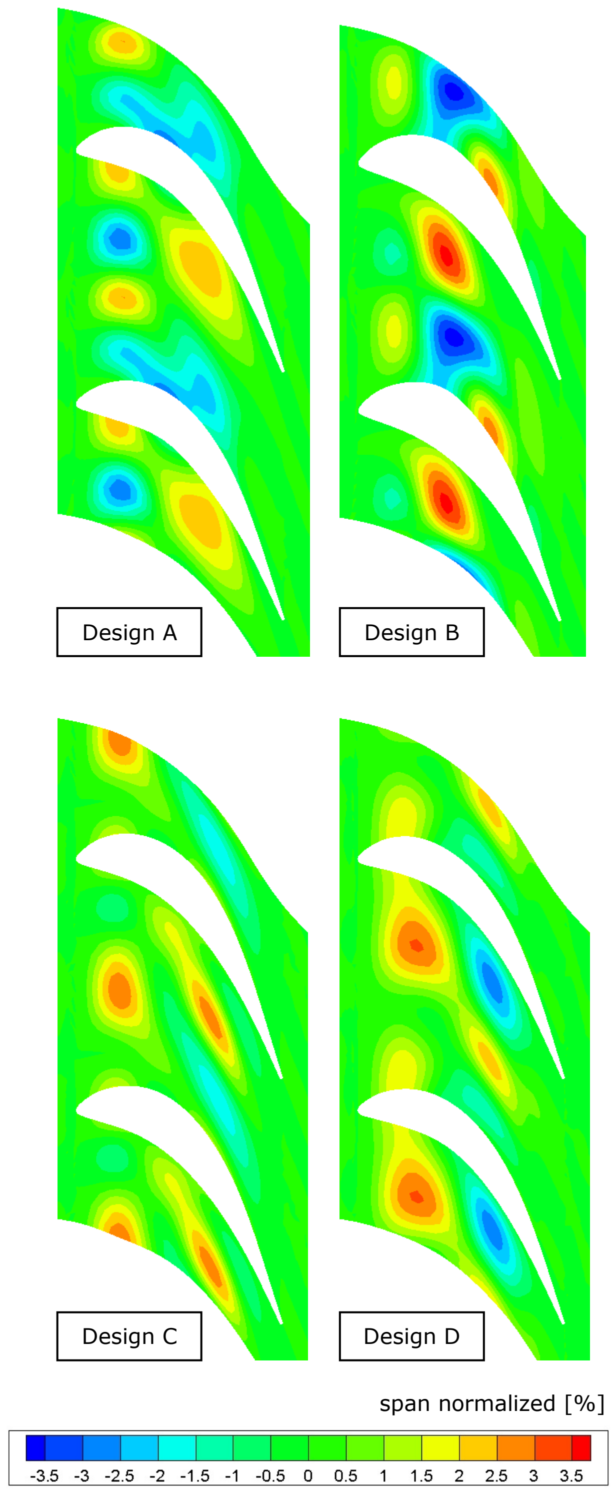

Fig. 7 Endwall contours of chosen designs

The second design features the lowest value of SKE3 with a reduction of 13.7%. By this design all loss values, which indicate the losses that are expected to occur downstream of the evaluation plane have been reduced. It is also the only design within these four, which has improved the mixing losses. However, all values of the upstream losses have been increased.

Design C shows a reduction in turbulent kinetic energy of 3.4 %. All other loss values have been increased.

The fourth design improves the kinetic energy loss by 0.8%. In this design no unified tendency can be found in the distinction between upstream losses and expectable downstream losses. This design also shows an entropy increase, although the correlation between the geometrical parameters and the KE_{loss} in fig. 4 are equivalent to the Δs_{io} correlations. This clearly shows that the KE_{loss} is not a suitable optimization parameter, since the isentropic reference enthalpy depends on the static pressure in the outlet evaluation plane.

None of the designs leads to a reduction of all loss values. These results therefore demonstrate that the reduction of secondary flow losses does not consequently lead to a reduction of the overall losses. The absence of this coherence is also shown by the radial distribution of the total pressure losses in fig. 8 and the exit angle in pitchwise direction in fig 9. The peak values of the total pressure loss at 13% and 82% are associated with the secondary flow losses. As expected, the reduction of the SKE values by Designs B and C leads to a reduction of the secondary losses. However, this improvement is attended by an increase of the losses in the adjacent regions of between 60% and 80% as well as 15% and 25% of the passage height.

Design A shows a contrary behavior. The secondary flow losses have been increased, while the profile losses have been improved locally, leading to a slight benefit in overall loss.

According to this, the reduced deflection of the flow at 12% and 85% span caused by the secondary flow is augmented in the case of design A and diminished in the case of design B.

The axial distribution of the entropy as a difference to the baseline is presented in fig. 10. The diagram shows that all modified designs incur a higher entropy production of up to 90% of the vane passage. As has been mentioned previously, a small separation bubble occurs in this region. Design A and Design C seem to have a beneficial impact on the losses produced by the separation bubble. Additionally, Designs A, B and C show a reduction in the mixing losses downstream of the evaluation plane at 1.182% of the axial chord, which is not in line with the calculated mixing losses. Since only the Euler equations are solve in the method of calculating the mixing losses, turbulent effects modeled by an additional viscosity cannot be taken into account. Therefore, care should be taken when evaluating the mixing losses as expectable downstream losses.

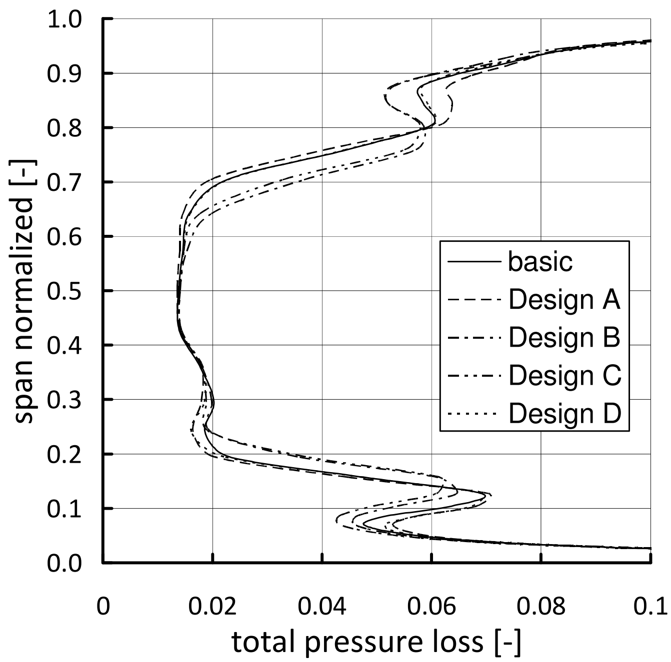

Fig. 8 Radial distribution of the total pressure loss

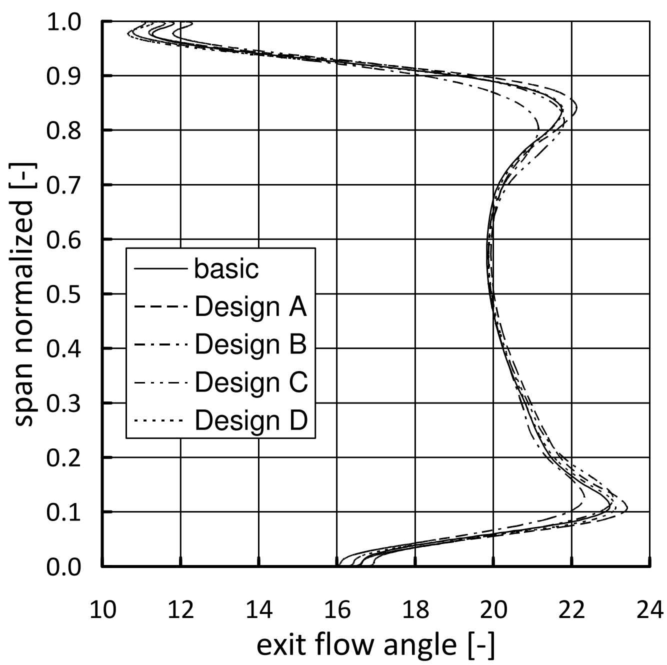

Fig. 9 Radial distribution of the exit flow angle in the pitchwise direction

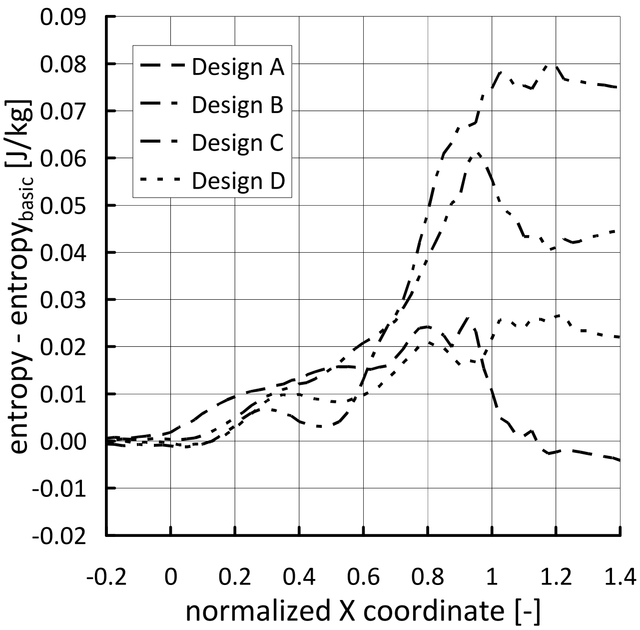

Fig. 10 Axial distribution of entropy as a difference to the baseline design

The effect of the three-dimensional design on the profile load is shown in fig. 11 in terms of an axial distribution of the isentropic Mach number. The profile loading of design B at 10% and 90% normalized span is typical for non-axisymmetric endwall contours. In the first 50% of the axial chord, the flow is decelerated resulting in a diminished cross-passage pressure gradient. After a short acceleration period, the positive pressure gradient at the rear part of the passage is decreased compared to the baseline design. This modification leads to an increased cross passage pressure gradient in the front part and a homogenized static pressure distribution at the throat of the passage.

Design A again shows a contrary distribution. This design supports a local aftloading of the vane, resulting in the increase of secondary flow as shown above.

The effect of the designs on the separation bubble can be found at 50% normalized span. Since there is a laminar-turbulent separation bubble, the decreasing influence of Design B on the length of the separation bubble is due to higher turbulence production. In consequence of the higher turbulence production increased profile losses occur.

CONCLUSIONS

The correlation matrix is a useful approach to identify geometrical parameters with a significant effect on the flow pattern. As has been shown, the geometrical parameters affect the aerodynamic parameters with a varying sensitivity. Since the dependence of different loss values is found in different geometrical parameters, it can be concluded that different geometrical design parameters fulfill different tasks within a three-dimensional vane design. After the clarification of the main deficits of the flow, the correlation matrix can be used to manipulate the flow to a desired result.

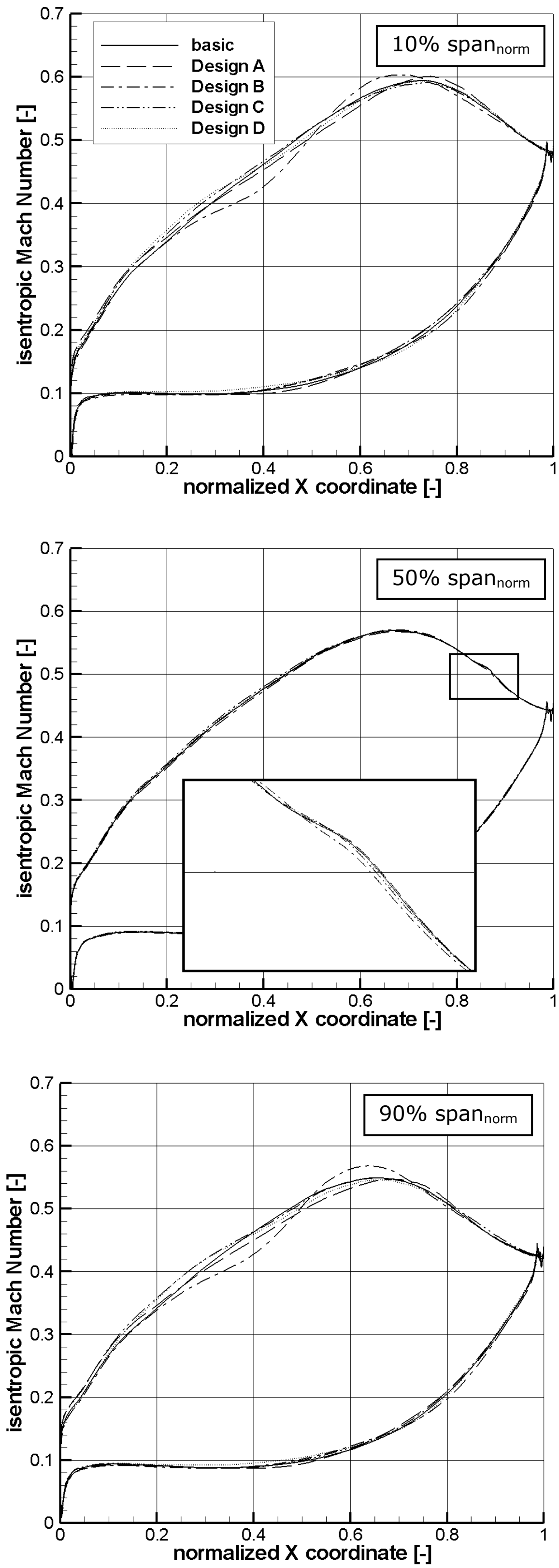

Fig. 12 Axial distribution of isentropic Mach number at 10%, 50% and 90% normalized span

In the flow conditions presented in this paper a separation bubble occurs on the suction side of the vane. Although the intention of three-dimensional vane designs is usually to reduce the secondary flow, better results have been achieved by reducing the losses associated with the separation bubble. Due to the fact that the geometry which provided reduced losses of the separation bubble showed an increase of secondary energy, the reduction of both sources of loss seems to be contradictory. Non-axisymmetric endwall contouring should be integrated early in the design process to compensate this behavior by profile modifications.

ACKNOWLEDGEMENTS

The results presented in this paper are gained from the project “3D-Turbinengestaltung”. This project is funded by the “Forschungsvereinigung für Verbrennungskraft-maschinen e.V.“ (FVV). The authors would like to express their gratitude to the FVV and the work group for their support and for the possibility to publish the results.

REFERENCES

[1] Rose M.G., 1994, “Non-Axisymmetric Endwall Profiling in the HP NGV´s of an Axial Flow Gas Turbine”, 94-GT-249, ASME 1994, The Hague, Netherlands

[2] Harvey N.W., Rose M.G., Taylor M.D., Shahpar S., Hartland J., Gregory-Smith D.G., 1999, “Non-Axisymmetric Turbine End Wall Design, Part I Three-Dimensional Linear Design System”, 99-GT-337, ASME 1999, The Hague, Netherlands,

[3] Hartland J. Gregory-Smith D., 2002, “A Design Method for the Profiling of End Walls in Turbines”, GT-2002-30433, ASME 2002, Amsterdam, Netherlands

[4] Ingram G., Gregory-Smith D., Harvey N., 2004, “Investigation of a Novel Secondary Flow Feature in a Turbine Cascade with End Wall Profiling”, GT2004-53589, ASME 2004, Vienna, Austria

[5] Brennan G., Harvey N.W., Rose M.G., Fomision N., Taylor M.D., 2001, “Improving the Efficiency of the Trent 500 HP Turbine using Non-Axisymmetric End Walls, Part 1: Turbine Design”, 2001-GT-0444, ASME 2001, New Orleans, USA

[6] Rose M.G., Harvey N.W., Seaman P., Newman D.A., McManus D., 2001, “Improving the Efficiency of the Trent 500 HP Turbine using Non-Axisymmetric End Walls, Part 2: Experimental Validation”, 2001-GT-0505, ASME 2001, New Orleans, USA

[7] Harvey N.W., Brennan G., Newman D.A., Rose M.G., 2002, “Improving Turbine Efficiency using Non-Axisymmetric End Walls, Validation in the Multi-Row Environment and with Low Aspect Ratio Blading”, GT-2002-30337, ASME 2002, Amsterdam, Netherlands

[8] Pioske C., 1998, “3D-Gestaltungskonzepte für Turbinenleiträder unter besonderer Berücksichtigung des Sekundärströmungsverhaltens“, PhD Thesis, RWTH Aachen University, Germany

[9] Nagel M.G., Fottner L., Baier R.-D., 2001, “Optimisation of Three Dimensionally Designed Turbine Vanes and Side Walls”, IS-2001-1058, ISABE 2001, Bangalore, India

[10] Nagel M.G., Baier R.-D., 2003, “Experimental verified numerical Optimisation of a 3D-parametrised Turbine Vane with non-axisymmetric End Walls”, GT2003-38624, ASME 2003, Atlanta, USA

[11] Schuepbach P., Rose M.G., Gier J., Raab I., Germain T., Abhari R., 2009, “Non-axisymmetric end wall profiles including fillet radii in a 1.5 stage axial flow turbine”, 8th European Conference on Turbomachinery: Fluid Dynamics and Thermodynamics 2009, Graz-Austria

[12] Poehler T., Gier J., Jeschke P., 2010, ”Numerical and Experimental Analysis of the Effects of Non-Axisymmetric Contoured Stator Endwalls in an Axial Turbine”, GT2010-23350, ASME 2010, Glasgow, Scotland

[13] Restemeier M., Guendogdu Y., Gier J., Jeschke P., 2011, ”Numerical and Experimental Analysis of the Effect of Variable Vane Row Spacing in a Subsonic Axial Turbine”, GT2011-45637, ASME 2011, Vancouver, Canada

[14] Rose M.G., Harvey N.W., 1999, ”Turbomachinery Wakes: Differential Work and Mixing Losses”, Journal of Turbomachinery, January 2000, Volume 122

[15] Hartung, Joachim, 1999, ”Statistik”, Oldenbourg Verlag